Spatially resolved characterization of heavy ion irradiated crystals using static field gradient nuclear magnetic resonance

2008 J. Phys.: Condens. Matter 20 275236

(http://iopscience.iop.org/0953-8984/20/27/275236)

J. Phys.: Condens. Matter **20** (2008) 275236 (4pp) doi:10.1088/0953-8984/20/27/275236

Spatially resolved characterization of heavy ion irradiated crystals using static field gradient nuclear magnetic resonance

H Stork[1], A Hamburger[1], A Gädke[1], F Fujara[1] and K Schwartz[2]

[1] Institut für Festkörperphysik, TU Darmstadt, Hochschulstraße 6, 64289 Darmstadt, Germany
[2] Gesellschaft für Schwerionenforschung (GSI), 64291 Darmstadt, Germany

E-mail: HolgerStork@gmx.de

Received 15 February 2008, in final form 20 March 2008
Published 6 June 2008
Online at stacks.iop.org/JPhysCM/20/275236

Abstract
Static magnetic field gradient NMR has been used for one-dimensional spatial ^{19}F spin–lattice relaxation profile studies (resolution of the order of 10 μm) in a LiF crystal irradiated with U ions. Technical aspects of the use of large static magnetic field gradients are discussed as well as a special data acquisition mode allowing for effectively measuring spatially resolved spin–lattice relaxation rates as low as 10^{-3} s^{-1}. In addition to the expected enhanced spin–lattice relaxation rate within the ion range, also an enhanced rate beyond the ion range has been found.

1. Introduction

The present work deals with the use of a spatially resolved nuclear magnetic resonance (NMR) method for the investigation of heavy ion radiation damage in ionic crystals. Radiation damage studies by magnetic resonance spectroscopy (NMR and EPR) were started in the 1950s. In thermal neutron irradiated LiF, radiolysis products were observed—fluorine molecules by means of NMR [1, 2] and Li colloids by means of EPR [3]. Metallic Li colloids were observed by means of NMR in LiF irradiated with fast electrons [4] and both NMR and EPR were applied in the study of heavy ion induced defects in LiF crystals [5, 6]. Regardless of the kind of radiation, a correlation between the nuclear spin–lattice relaxation rate T_1^{-1} and the paramagnetic defect density was experimentally tested in these studies and the dynamical and thermal properties of the defects were investigated through their temperature and field dependence. As a mechanism the authors suggested relaxation at radiation induced paramagnetic F-centres and magnetization transport towards these centres due to spin diffusion.

When comparing the wealth of NMR results with those from other relevant spectroscopic methods (e.g. optical absorption [7] and luminescence spectroscopy [8], scanning force microscopy [9] and profilometry (swelling) [10]) one should note several aspects. First, there are several NMR methods [11] able to detect structural properties (NMR spectroscopy) as well as dynamical processes (NMR relaxometry, NMR diffusometry) while most other methods record static structural information (i.e., only the defect type). A smart combination of various available NMR methods (relaxometry, spectroscopy, diffusometry) might have a high potential in identifying both geometry and timescale for defect dynamics. Second, unfortunately, the NMR technique is a quite insensitive method and can by no means compete with the EPR technique and, especially, optical spectroscopy. However, as will be discussed below, nuclear spin diffusion may strongly enhance the ability of NMR studies to detect radiation induced defects. And third, so far NMR has never been used to reveal spatially resolved information on radiation damage with the required resolution on the μm scale.

As far as homogeneously irradiated samples are concerned, spatial resolution is not needed. However, heavy ions typically have an energy dependent penetration depth and a complex damage morphology (depending on the energy loss of the ions). In this study, depth dependent NMR relaxation measurements on LiF crystals irradiated with heavy ions are presented for the first time. The technique used is known as stray-field imaging, microimaging or microtomography [11, 12].

2. Experimental details

A LiF single crystal ($5 \times 5 \times 0.4$ mm^3) has been irradiated at the UNILAC linear accelerator of GSI Darmstadt with ^{238}U ions of 2640 MeV at a fluence of 10^{11} ions cm^{-2}. Their mean spatial

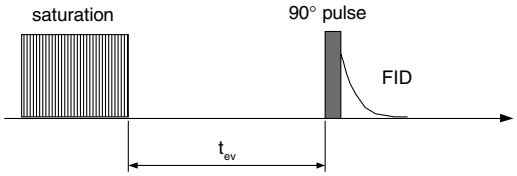

Figure 1. Pulse sequence used for the spatially resolved NMR measurements. First, the magnetization is destroyed by a sequence of eight 90° pulses. After the evolution time t_{ev} the actual value of the nuclear magnetization, relaxing back towards its thermal equilibrium value, is read out from the amplitude of a free induction decay (FID) signal following a single 90° pulse.

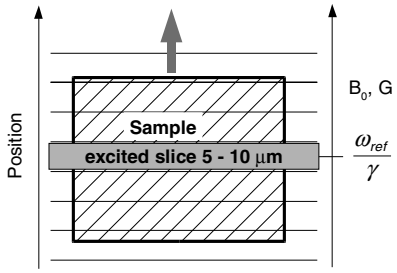

Figure 2. Sample moving in a magnetic field gradient (G). The grey arrow shows the direction of the movement. The horizontal lines symbolize isolines of the magnetic field B_0. The excited slice remains at the position corresponding to the reference frequency ω_{ref}.

energy loss density was 27.2 keV nm^{-1} and their penetration depth about 95 μm.

The NMR measurements have been performed using a home-built specialized NMR spectrometer usually being used for static field gradient diffusometry [13]. The experiments have been carried out at a magnetic field of 3.74 T and a magnetic field gradient of 74.3 T m^{-1}. At corresponding positions the isolines of the magnetic field are sufficiently parallel to allow μm resolution. The resonant nucleus was ^{19}F (resonance frequency 149.6 MHz) and the experimental temperature was set to (295 $\pm$ 2) K. For measuring the nuclear spin–lattice relaxation rate, a 'saturation–recovery' pulse sequence (figure 1) was chosen. It consists of a burst of pulses aiming for saturating the nuclear magnetization, followed by a variable evolution time t_{ev} and a rectangle shaped probing 90° pulse. (Since the flip angle is not well defined in an inhomogeneous field we denote as '90° pulse' a pulse with a length maximizing the signal intensity.) Due to a narrow excitation bandwidth it has been possible, instead of using echoes, to record the signal from the free induction decay (FID). The amplitude $S(t_{ev})$ of the FID invoked by the probing pulse is recorded as a function of t_{ev}. By fitting the test function $S(t_{ev}) = A + B\exp(-t_{ev}/T_1)$ to the measured FID amplitudes, the spin–lattice relaxation rate T_1^{-1} is determined.

In a magnetic field gradient (G) the excited slice thickness of a rf pulse with duration t_p is $\Delta z = \frac{1}{\gamma G t_p}$ (with ^{19}F gyromagnetic ratio γ). For our experiments the thickness of the excited slice was 7.5 μm according to a pulse length of 45 μs. The limiting factor for the pulse length is the short T_2 of a few tens of μs.

The position of the sample can be changed by a stepping motor parallel to the magnetic field gradient (figure 2). The home-built stage allows repositioning precision within 2 μm. The precision in long term measurements is limited to about 10 μm due to thermal expansion.

When the sample moves, the excited slice passes across the sample. This results in spatially resolved signal intensity profiles. A typical set of such profiles—with the evolution time t_{ev} being the parameter—for the irradiated LiF sample of 400 μm thickness is shown in figure 3. From these data it is straightforward to obtain spatially resolved magnetization–recovery curves and thereby spin–lattice relaxation rates (see figure 5).

In order to limit the measurement time, a sampling scheme has been applied as shown in figure 4. The idea is to read out the signal intensities consecutively at many positions before repeating the whole cycle for signal averaging instead of accumulating the signal at each one position and thereby always waiting the evolution time t_{ev}. Therefore the pulse sequence in figure 1 has been slightly modified for long evolution times. Before the first accumulation the magnetization is destroyed at several positions by a saturation comb. After the evolution time the signal intensity is measured and the magnetization destroyed by a following saturation sequence at the same positions. In order to exclude influences of the pulse on neighbouring positions, the order has been staggered. The minimum distance Δs between positions which are set directly one after another has been determined experimentally to be about 67 μm. From figure 5 it is seen that for smaller steps (33 μm and below) the signal amplitude gradually decreases and the profile becomes distorted. However, figure 6 shows that this does not simultaneously influence the relaxation rate profile, since for a step size of 33 μm there is no significant difference in spin–lattice relaxation rate T_1^{-1} as compared to 67 μm. The sampling scheme obviously only works when the time needed for the transfer of the sample is less than the evolution time. To extend the scope of this method, the distance has been divided into two (as exemplified in figure 4), four or eight sections.

For large values of t_{ev} the number of accumulations has been reduced. The applied sampling scheme decreases the measurement time by about two orders of magnitude. It has been implemented in the home-written spectrometer control platform 'DArmstadt MAgnetic Resonance Instrument Software' (DAMARIS) [14] which provides the necessary flexibility. Another important factor for measurement time reduction has been the use of newly designed flat rf coils which, due to the optimized filling factor, lead to an increase of the signal to noise ratio by approximately a factor of 2 to 3 as compared to that for conventional solenoid rf coils. A detailed account of the design and the invoked gain in the signal to noise ratio of those flat rf coils will be the subject of a forthcoming publication. Using these concepts, the typical duration of a position dependent nuclear spin–lattice relaxation rate experiment on an irradiated LiF crystal has been less than two days.

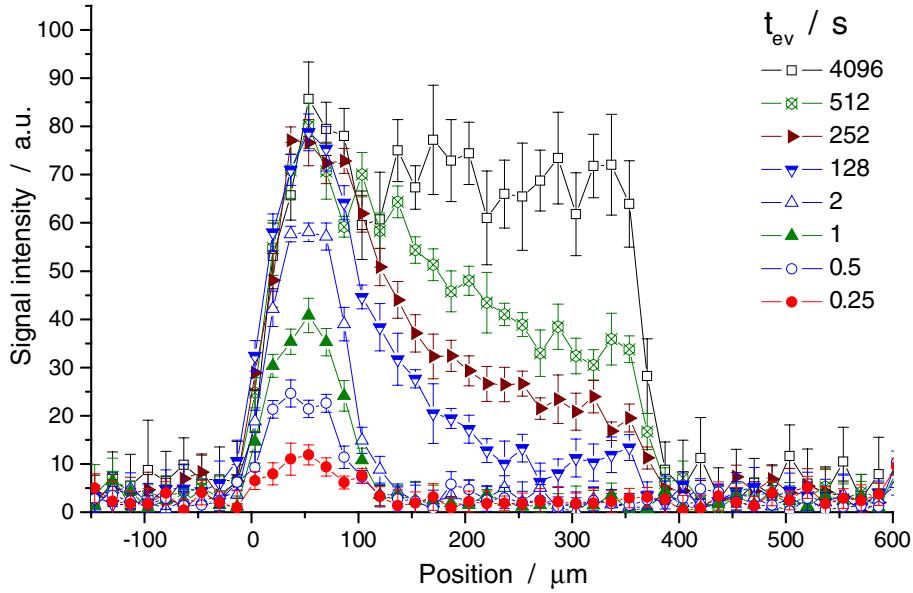

Figure 3. Signal intensity profiles for selected evolution times t_{ev}. For $t_{ev} \leqslant 2$ s 32, for 4 s $\leqslant t_{ev} \leqslant 1024$ s 16, for $t_{ev} = 2048$ s 8 and for $t_{ev} = 4096$ s 4 accumulations have been taken, respectively.

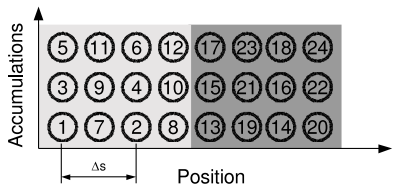

Figure 4. Applied sampling scheme. The numbers mark the chronological order of the experiments. For instance: at a given position three accumulations have been performed such that '1' is followed by '3' and by '5'. In the meantime experiments have been performed at other positions, the step width being Δs. In any case the correct time interval t_{ev} in between subsequent accumulations at a given position (for instance in between '1' and '3') has been ensured. In the figure, two sample sections are scanned consecutively.

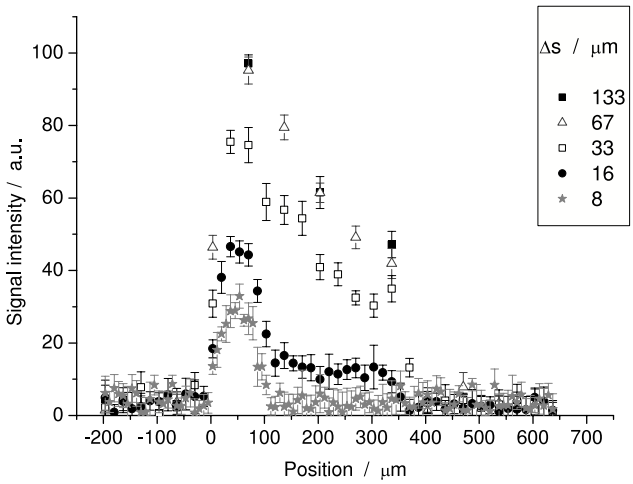

Figure 5. Signal intensity profiles for several step widths Δs. In each case 16 accumulations have been taken. The evolution time was set to $t_{ev} = 512$ s.

3. Results and discussion

The above presented experiments result in position dependent spin–lattice relaxation rates T_1^{-1} (see figure 6). There has been some ambiguity in assigning the zero position, i.e. the crystal surface. In figure 3, this zero position has been pragmatically defined by demanding that the fully relaxed signal intensity reaches 25% of the maximum intensity. The resolution is not limited by the slice thickness but by the flatness of the crystal surface. In the relaxation profiles, three regions can be distinguished from each other. First, the heavy ion irradiated zone (below about 100 μm) can easily be identified due to the significantly larger relaxation rate. Second, there is a transition region up to approximately 130 μm where the relaxation rates decrease rapidly with increasing depth. Since the ion penetration depth (95 μm) is defined within less than 3 μm only [15], we cannot exclude that the width of the transition region is caused by a not well defined crystal surface. In any case, in this transition region the signal intensity profiles show multiexponential contributions (figure 7). Therefore the monoexponential model fits the data only poorly, which is reflected by the increased error bars in the transition region. In the third region (above about 130 μm) there is a gradient in the relaxation rate decreasing gradually towards the background relaxation rate of the non-irradiated sample. According to [16], in the zone beyond the ion range the relaxation might be due to the presence of paramagnetic F-centres created by the bremsstrahlung (x-rays) from δ electrons in the ion tracks. However, the increased relaxation rate observed in the nominally non-irradiated zone, denoted above as the third region, has never been observed before.

4. Summary and conclusions

One-dimensional NMR microimaging (microtomography) has been introduced as a new method for the investigation of heavy

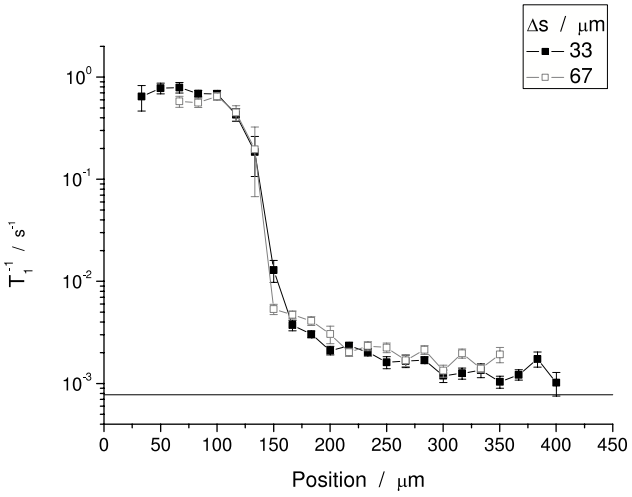

Figure 6. Spatially resolved spin–lattice relaxation rates T_1^{-1} for two step widths Δs of 67 μm (open symbols) and 33 μm (full symbols). The horizontal line symbolizes the spin–lattice relaxation rate of the non-irradiated LiF sample.

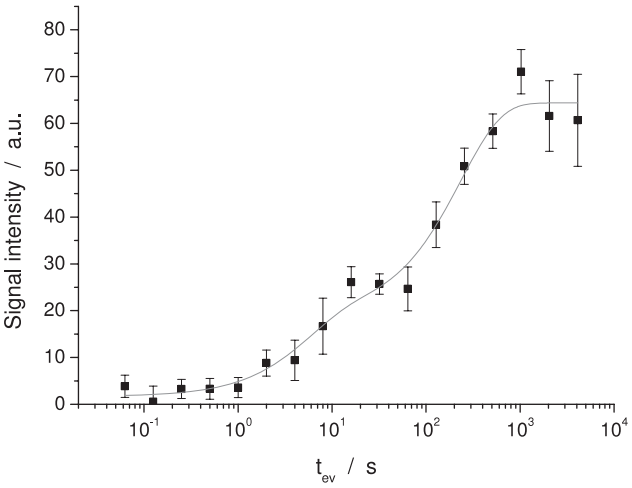

Figure 7. Signal intensity versus evolution time t_{ev} at position 120 μm. The fit curve is biexponential with relaxation times $T_1^a = (5.4 \pm 2.9)$ s and $T_1^b = (235 \pm 52)$ s.

ion radiation damage in solids. A spatial resolution of the order of 10 μm has been achieved. In the case of U irradiated LiF crystals, spatially resolved ^{19}F spin–lattice relaxation rates turn out to be sensitive to the paramagnetic defect density gradient along the ion track direction. Three regions can be identified and distinguished from each other: first, the part within the ion range (down to about 95 μm penetration depth); second: a transition region (95–130 μm); third, the deep crystal interior (beyond 130 μm) not penetrated by the ions. In the first region the relaxation rate turns out to be raised by about three orders of magnitude compared with non-irradiated LiF. A relaxation gradient in the third region indicates the presence of paramagnetic defects due to secondary x-rays.

This paper marks the starting point of an extended NMR project. Even limiting ourselves to the currently available irradiated LiF crystals, a couple of other experiments remain to be done: LiF samples irradiated with different ion types, energies and fluences should be investigated. An important scientific question is that of the defect saturation. Does it depend on the ion type, on the energy, on the energy loss density dE/dz? For better specifying the defect type and the relaxation mechanism, also spatially resolved ^{7}Li relaxation measurements are envisaged, and NMR spectroscopy should be applied looking for structural defects, e.g. the possible appearance of F_2 molecules. In the longer term, it will be a challenge to study the frequency dependence of relaxation rates (spatially resolved field cycling) and the (spatially resolved) annealing behaviour. Obviously, also EPR and optical absorption experiments should be performed, thus not only hoping to obtain an independent F-centre concentration determination but also to learn about structural details of these centres.

There are excellent perspectives that spatially resolved NMR might lead to significant progress in the understanding of heavy ion radiation effects in ionic solids.

Acknowledgments

The authors would like to thank R Neumann (GSI) for his encouragement in initiating this project, C Trautmann and B Schuster (GSI) for their support in irradiating the crystals and O Kanert (Dortmund) for fruitful discussions.

References

[1] Ring P J, O'Keefe J G and Bray P J 1958 *Phys. Rev. Lett.* **1** 453
[2] Hooper D H O and Bray P J 1966 *J. Phys. Chem. Solids* **27** 147
[3] Kaplan R and Bray P J 1963 *Phys. Rev.* **129** 1919
[4] Zogal O J, Beuneu F and Vajda P 2002 *Phys. Rev.* B **66** 064101
[5] Klempt T, Schweizer S, Schwartz K, Kanert O, Suter D, Rogulis U and Spaeth J-M 2001 *Radiat. Eff. Defects Solids* **155** 159
[6] Klempt T, Kanert O and Suter D 2003 *Phys. Status. Solidi* b **236** 151
[7] Davidson A-T, Schwartz K, Comins J D, Kozakiewicz A G, Toulemonde M and Trautmann C 2002 *Phys. Rev.* B **66** 214102
[8] Lushchik A, Lushchik Ch, Schwartz K, Vasil´chenko E, Papaleo R, Sorokin M, Volkov A E, Neumann R and Trautmann C 2007 *Phys. Rev.* B **76** 054114
[9] El-Said A S, Neumann R, Schwartz K and Trautmann C 2002 *Surf. Coat. Technol.* **158/159** 522
[10] Trautmann C, Toulemonde M, Costantini J M, Grob J J and Schwartz K 2000 *Phys. Rev.* B **62** 13
[11] Kimmich R 1997 *NMR Tomography, Diffusometry, Relaxometry* (Heidelberg: Springer)
[12] MacDonald P J 1997 *Prog. Nucl. Magn. Reson. Spectrosc.* **30** 69
[13] Chang I, Fujara F, Geil B, Hinze G, Sillescu H and Tölle A 1994 *J. Non-Cryst. Solids* **172–174** 674
[14] Gädke A, Rosenstihl M, Schmitt C, Stork H and Nestle N 2007 *Diffus. Fundam.* **5** 6.1–6.9
[15] Ziegler J F, Ziegler M D and Biersack J P 2006 http://www.srim.org/
[16] Vasil´chenko E, Kudryavtseva I, Kärner T, Lushchik A, Nagirnyi V and Nakonechnyi S 2006 *13th Int. Conf. on Radiation Physics and Chemistry of Inoraganic Materials (Tomsk)* ed V Lisitsyn and V Lopatin pp 11–114